Superposing pure quantum states with partial prior information

Shruti Dogra,[1,2,*] George Thomas,[1,†] Sibasish Ghosh,[1,‡] and Dieter Suter[2,§]

[1]*Optics and Quantum Information Group, The Institute of Mathematical Sciences, HBNI, CIT Campus, Taramani, Chennai 600113, India*

[2]*Fakultät Physik, Technische Universität Dortmund, D-44221 Dortmund, Germany*

(Received 9 March 2017; revised manuscript received 31 October 2017; published 29 May 2018)

The principle of superposition is an intriguing feature of quantum mechanics, which is regularly exploited in many different circumstances. A recent work [M. Oszmaniec *et al.*, Phys. Rev. Lett. **116**, 110403 (2016)] shows that the fundamentals of quantum mechanics restrict the process of superimposing two unknown pure states, even though it is possible to superimpose two quantum states with partial prior knowledge. The prior knowledge imposes geometrical constraints on the choice of input states. We discuss an experimentally feasible protocol to superimpose multiple pure states of a d-dimensional quantum system and carry out an explicit experimental realization for two single-qubit pure states with partial prior information on a two-qubit NMR quantum information processor.

DOI: 10.1103/PhysRevA.97.052330

I. INTRODUCTION

According to the postulates of quantum theory, it is generally possible to generate superpositions of arbitrary pairs of pure states of a quantum system unless there exists a superselection rule [1,2]. However, a recent study showed that there exists no general quantum protocol for creating superpositions of a completely unknown pair of pure quantum states [3,4]. The difficulty of superimposing unknown quantum states was first discussed in Ref. [3] in the context of quantum adders. Quantum states that are equivalent up to a global phase represent the same physical state. Therefore, the superposition of unknown quantum states that are equivalent, up to their global phases, may result in a relative phase between these states, and thus in different states. However, some partial prior knowledge about the states can be used to achieve the restricted type of superposition, as suggested in a recent work [4]. As shown in Ref. [4], two unknown quantum states $|\psi_1\rangle$ and $|\psi_2\rangle$ can be superposed if their overlaps with a reference state $|\chi\rangle$ are known and nonzero. For the superposition of two d-dimensional states, a tripartite system of dimension $2d^2$ is used. The corresponding state is initialized into $(a|0\rangle + b|1\rangle)|\psi_1\rangle|\psi_2\rangle$, with arbitrary complex coefficients a, b. This state is subsequently transformed by a three-party controlled-SWAP gate. Finally, two projection operators are constructed using the reference state $|\chi\rangle$ and its overlaps ($|\langle\chi|\psi_i\rangle|$) with the states to be superimposed. The application of these projectors generates a state proportional to $(a\kappa_2|\psi_1\rangle + b\kappa_1|\psi_2\rangle)$, where $\kappa_i = \langle\chi|\psi_i\rangle/|\langle\chi|\psi_i\rangle|$.

In general, for the sake of quantum computation, it may be useful to experimentally superpose unknown quantum states [5]. For the past few decades, there has been a growing interest for more feasible, robust experimental quantum computation models [6–9]. Experimental realization of superposition of unknown quantum states is significant, not only as a quantum computational task but also as a fundamental principle. There exist experimental techniques based on photons [10], nuclear spins [11], and superconducting qubits [12] that implemented the superposition protocol discussed in [4]. In Ref. [10], the superposition of two photonic states is realized. The controlled-SWAP implementation was a challenge here; therefore, an effective controlled-SWAP operation was implemented which includes postselection and is a nonunitary operation. Another work [11] presents the experimental implementation of the superposition protocol [4] using three nuclear spins, where the controlled-SWAP gate was implemented via numerically optimized pulses. This was followed by a three-qubit tomography and, subsequently, tracing out first and third qubits numerically to imitate projective measurements. A transmons-based implementation of Refs. [3,4] was realized on the IBM Quantum Experience [12]. This scheme implemented an optimal quantum circuit obtained using genetic algorithm techniques, but its operation is limited to specific input states.

The present work experimentally realizes a full protocol to perform the desired superpositions of pure states of a quantum system, addressing all the aspects discussed in Ref. [4]. The experiment-friendly superposition protocol discussed here overcomes the experimental inefficiencies reported in Ref. [11]. Moreover, this is a two-qubit-based experimental implementation to superpose two single-qubit states, contrary to the existing implementation that used three physical qubits [11]. The protocol is further generalized to superpose n higher-dimensional quantum states. A detailed comparison between our experimentally implemented protocol with that of existing experimental implementations in terms of the success probabilities is carried out. We also analyze the enhancement in the success probabilities associated with the desired superpositions for different prior information.

*Present address: Department of Physics, IIT Madras, Chennai, India; shrutidogra.iiserm@gmail.com

†georget@imsc.res.in

‡sibasish@imsc.res.in

§dieter.suter@tu-dortmund.de

The material in this paper is arranged as follows: theoretical development of the experiment-friendly superposition protocol is described in Sec. II. Further, experimental implementation using a system of two nuclear spins is given in Sec. III. The extension of our scheme to superpose n higher-dimensional quantum states is discussed in Sec. IV. The comparison of the success probabilities with respect to the previously implemented superposition protocol [11] and its enhancement subject to prior information are discussed in Sec. V. This is followed by the concluding Sec. VI.

II. THEORETICAL SCHEME

Let us consider the superposition of two arbitrary states $|\Psi_1\rangle$ and $|\Psi_2\rangle$, with desired weights of superposition (a and b) and whose respective inner products $\langle\chi|\Psi_i\rangle$ with a known referential state $|\chi\rangle$ are given. It is well known that a state $|\Psi\rangle$ and $e^{i\gamma}|\Psi\rangle$ represent the same physical states, despite different values of the overall phase "γ." However, the superposition of these states depends upon the values of the respective overall phases of the constituent states. While the global phase of a state is intangible, it is possible to determine the overall phase of a state with respect to a reference state. Here we use the partial prior information given in terms of the inner products $\langle\chi|\Psi_i\rangle$ to obtain the overall phase factors, $e^{i\gamma} = \langle\chi|\Psi_i\rangle/|\langle\chi|\Psi_i\rangle|$. The details of the protocol are worked out in the following stanzas. Thus, for the class of states $|\Psi_i\rangle = e^{i\gamma_i}|\psi_i\rangle$ that are equivalent to each other up to an overall phase, $\gamma_i \in [0,2\pi]$, the desired superimposed state may be written as $a|\psi_1\rangle + b|\psi_2\rangle$.

Beginning with an explicit analysis for the superposition of two single-qubit pure states, we consider a system of two coupled spin-1/2 particles (denoted here as A and X) under the action of a Hamiltonian,

$$H = -\Omega_A A_z \otimes \mathbb{I}_X - \Omega_X \mathbb{I}_A \otimes X_z + J A_z \otimes X_z, \quad (1)$$

where Ω_A (Ω_X) is the resonance frequency and A_z (X_z) is the z component of angular momentum for spin A (X). J represents the scalar coupling constant. $|0\rangle_A, |1\rangle_A$ ($|0\rangle_X, |1\rangle_X$) are the eigenvectors of A_z (X_z) with eigenvalues $+1/2, -1/2$ respectively. The single-qubit pure states of our system are encoded in the eigenbasis $\{|00\rangle, |01\rangle, |10\rangle, |11\rangle\}$ of the Hamiltonian H. We use the subspace spanned by $|00\rangle, |01\rangle$ of H to store the single-qubit input state $|\Psi_1\rangle = c_{00}|0\rangle + c_{01}|1\rangle$, where $|c_{00}|^2 + |c_{01}|^2 = 1$, while the subspace spanned by the two remaining levels is used to store the input state vector $|\Psi_2\rangle = c_{10}|0\rangle + c_{11}|1\rangle$, where $|c_{10}|^2 + |c_{11}|^2 = 1$. The state of the two-qubit system ($A + X$) is then

$$|\Psi\rangle' = a|0\rangle \otimes e^{i\gamma_1}|\psi_1\rangle + b|1\rangle \otimes e^{i\gamma_2}|\psi_2\rangle, \quad |a|^2 + |b|^2 = 1, \quad (2)$$

where a and b are the weights of the superposition. In Eq. (2), the first qubit is the ancilla and the second qubit is the system qubit. The superposition protocol that we propose here generates the desired superimposed state, irrespective of the values of phase factors (say, $e^{i\gamma_j}$ with jth input state) [4]. Given any fixed state $|\chi\rangle$ of the system qubit (such that $\langle\chi|\psi_i\rangle \neq 0$), prior knowledge of the inner products $\langle\chi|\psi_1\rangle$ and $\langle\chi|\psi_2\rangle$ is exploited to find the phases $e^{i\gamma_j}$. Using this information, we construct a phase gate ($e^{i\theta_z(A_z\otimes\mathbb{I}_X)}$), which implements a z rotation on the first qubit by an angle $\theta_z = \frac{\gamma_1-\gamma_2}{2}$, leading to the state

$$|\Psi\rangle'' \equiv e^{i\frac{\gamma_1+\gamma_2}{2}}(a|0\rangle|\psi_1\rangle + b|1\rangle|\psi_2\rangle). \quad (3)$$

Thus the phases with the individual single-qubit states are modified and appear as an overall phase of the two-qubit state. In Appendix A, a detailed view of an alternative protocol is given to encode the states $|\psi_1\rangle, |\psi_2\rangle$ and to get rid of their phases $e^{i\gamma_1}, e^{i\gamma_2}$, respectively. Further, a Hadamard gate on the first qubit in Eq. (3) leads to the state (ignoring the overall phase $e^{i\frac{\gamma_1+\gamma_2}{2}}$)

$$|\Psi\rangle''' \equiv \frac{|0\rangle}{\sqrt{2}}(a|\psi_1\rangle + b|\psi_2\rangle) + \frac{|1\rangle}{\sqrt{2}}(a|\psi_1\rangle - b|\psi_2\rangle). \quad (4)$$

Depending upon the state of the first qubit, one can choose between the sum or difference of the single-qubit states $|\psi_1\rangle$ and $|\psi_2\rangle$: a measurement on the first qubit in the basis $\{|0\rangle, |1\rangle\}$ gives rise to the state $a|\psi_1\rangle + b|\psi_2\rangle$ of the second qubit (in the case of outcome $|0\rangle$), which is proportional to the desired superposed state $N_\psi(a|\psi_1\rangle + b|\psi_2\rangle)$ (N_ψ being the normalization constant) obtained with a success probability $N_\psi^2/2$. Thus, with the help of only one ancillary qubit, we are able to superpose two single-qubit states. Also, $e^{i\gamma_i}$ does not show up in the final superposed state, which implies that the overall phase factors of the constituent states do not alter the resultant superimposed state in this protocol.

In the present context, no-go theorems concerning the implementation of unknown quantum operations [13–15] are circumvented by using the general protocol, which creates "arbitrary" pairs of input states within the given constraints. It is important to note that no extra information regarding arbitrary pairs of input states is used further in the superposition protocol.

III. EXPERIMENTAL IMPLEMENTATION

The NMR pulse sequence to carry out weighted superposition of two single-qubit states is shown in Fig. 1, where the first channel corresponds to the ancillary qubit A and the second channel corresponds to the system qubit X (here labeled as ^{1}H and ^{13}C, respectively). The pulse sequence is divided into three blocks: initial, encoding, and superposition, as mentioned in Fig. 1. In the first block, system and ancillary qubits are jointly initialized in state $|00\rangle$. A single-qubit rotation by an angle 2δ about the $\hat{\hat{y}}$ axis is applied on the ancillary qubit, generating the state $a|00\rangle + b|10\rangle$ (with $a = \cos\delta$ and $b = \sin\delta$). The second block, labeled "encoding," encodes the arbitrary pair of single-qubit states. This is achieved by two two-qubit controlled operations that encode the second qubit with state $|\psi_1\rangle$ when the first qubit is in state $|0\rangle$, and with state $|\psi_2\rangle$ when the first qubit is in state $|1\rangle$. Each controlled operation is achieved by a controlled rotation of the second qubit by an angle $(\theta_j)_{n_j}$ where the state of the first qubit, $|j\rangle$ ($j \in \{0,1\}$), is the control. The axis of rotation $\hat{n}_j = \cos(\phi_j)\hat{y} + \sin(\phi_j)\hat{x}$. At the end of this step [labeled as (ii) in Fig. 1], the joint state of the system and ancilla is given by $a|0\rangle|\psi_1\rangle + b|1\rangle|\psi_2\rangle$, such that the encoded state $|\psi_j\rangle$ is parametrized by $\{\theta_{j-1}, \phi_{j-1}\}$ ($j = 1,2$). This encoded

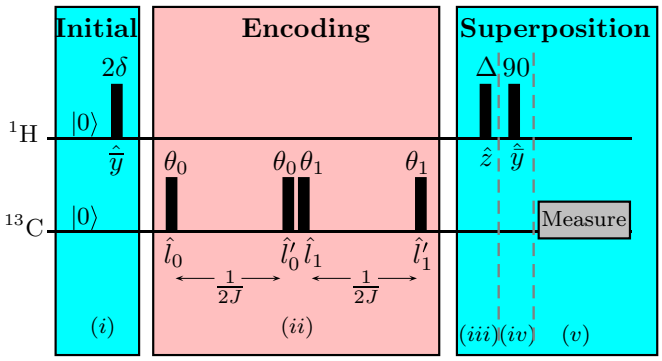

FIG. 1. NMR pulse sequence to obtain a superposition of two single-qubit states starting with the pseudopure state $|00\rangle$. The two channels show the operations on ancilla (^{1}H) and system qubits (^{13}C), respectively. Pulse sequence is divided into three parts, shown as separate blocks of different colors. Also, various steps are numbered from (i)–(v). The radio-frequency pulses are shown as rectangles, with the respective angles of rotation mentioned at the top and the axes of rotation specified at the bottom. The arbitrary rotation axes are $\hat{l}_0 = \cos(\frac{3\pi}{2}+\phi_0)\hat{x} + \sin(\frac{3\pi}{2}+\phi_0)\hat{y}$, $\hat{l}'_0 = \cos(\phi_0)\hat{x} + \sin(\phi_0)\hat{y}$, $\hat{l}_1 = \cos(\pi+\phi_1)\hat{x} + \sin(\pi+\phi_1)\hat{y}$, and $\hat{l}'_1 = \cos(\frac{\pi}{2}+\phi_1)\hat{x} + \sin(\frac{\pi}{2}+\phi_1)\hat{y}$. At the end of the sequence, a single-qubit measurement is performed on the system qubit.

two-qubit state is then fed into the block named "superposition," wherein possible overall phases of the arbitrary input states ψ_1 and ψ_2 are taken care of by applying a z pulse of angle $\Delta = \frac{\gamma_1-\gamma_2}{2}$ on the first qubit, leading to the state given in Eq. (3). This is followed by a pseudo-Hadamard gate on the ancillary qubit, which is a 90° pulse about the $\hat{\bar{y}}$ axis (along negative y direction), leading to the joint state of the system and ancilla as given in Eq. (4). A partial readout of the system qubit leads to the expected superposed state. In all the experiments, the referential state ($|\chi\rangle$) is chosen as $|0\rangle$.

As discussed in the theoretical scheme, the measurement consists of a projective measurement on the first qubit ($|0\rangle\langle 0| \otimes \mathbb{I}_{2X2}$), followed by a partial-trace operation that retains the state of the second qubit. The measurement applies therefore *only* to the subspace spanned by the eigenvectors $|00\rangle$ and $|01\rangle$ of H. Experimentally, the corresponding information is contained in the coherence between these two states. Thus the final superposed state is recovered from a two-dimensional subspace by partial quantum state tomography. This approach may also be useful in different experiments as a replacement of projective readout. The desired single-qubit density operator is obtained by a set of two operations: (i) direct readout, to obtain the information about the single-quantum coherence between states $|00\rangle - |01\rangle$ and (ii) application of a gradient (G_z), followed by a 90° pulse about the y axis $[(\frac{\pi}{2})^2_y]$ on the second qubit, to obtain the relative populations of the energy levels $|00\rangle$ and $|01\rangle$. In both cases, we observe the spectral line corresponding to transition $|00\rangle - |01\rangle$. The resultant single-qubit density operator is un-normalized in this protocol. The normalization constant for the desired part of the density operator can be obtained experimentally by measuring the sum of the populations of states $|00\rangle$ and $|01\rangle$. This is achieved by applying a gradient to dephase the coherences, followed by a spin-selective 90° pulse on the first qubit $[G_z(\frac{\pi}{2})^1_y]$. A readout of the resultant NMR spectrum of the first qubit provides the normalization constant for the desired subspace. This normalization factor is then used to completely characterize the final state density operator of the superposed state.

The pulse sequence shown in Fig. 1 is implemented experimentally on a sample consisting of ^{13}C labeled chloroform in deuterated acetone. The experiments were performed on a 500 MHz Bruker Avance II NMR spectrometer with a QXI probe head. All pulses were high-power, short-duration rf pulses applied to the ^{1}H and ^{13}C spins on resonance. The scalar coupling constant $J = 215$ Hz. The spin-spin relaxation times (T_2^*) of the ^{1}H and ^{13}C spins were 540 and 170 ms, respectively. Nuclear spin systems at thermal equilibrium are in a mixed state. The system was thus initialized into a pseudopure state $|00\rangle$ by spatial averaging [16] with a fidelity of 0.999. Starting from this pseudopure state, various pairs of single-qubit states ($|\psi_1\rangle$ and $|\psi_2\rangle$) were encoded on a two-qubit system, as described earlier.

In order to ensure the accuracy of this experimental implementation, two-qubit density operators were tomographed at the end of steps (ii) and (iv) of the pulse sequence (Fig. 1), thus obtaining the state after encoding ($\rho_{\rm exp}^{(ii)}$) and the state before the measurement ($\rho_{\rm exp}^{(iv)}$), respectively. The two-qubit states were completely reconstructed with a set of four operations: $\{\mathbb{II}, \mathbb{IX}, \mathbb{IY}, \mathbb{XX}\}$, where $\mathbb{X}(\mathbb{Y})$ refers to a spin-selective 90° pulse along the $x(y)$ axis. The single-qubit density operator of the system qubit is obtained through two operations on the system qubit: $\{\mathbb{I}, G_z\mathbb{Y}\}$, where G_z is the nonunitary gradient implementation about the z axis. The resultant single-qubit reduced density operator is then normalized as described earlier in this section. The fidelity between the theoretically expected (ρ_t) and the experimentally obtained (ρ_e) states was measured using the following expression:

$$\mathcal{F} = \mathrm{Tr}(\rho_e\rho_t)/\sqrt{\mathrm{Tr}\left(\rho_e^2\right)\mathrm{Tr}\left(\rho_t^2\right)}. \tag{5}$$

Table I summarizes the results of various experiments, where columns 2 and 3 show the single-qubit pure states to be superposed, and column 5 contains the fidelity ($\mathcal{F}$) between

TABLE I. Summary of experimental results.

S. no.	Input state $\|\psi_1\rangle$	Input state $\|\psi_2\rangle$	$\frac{a}{b}$	$\mathcal{F}$
1	$\|0\rangle$	$\frac{1}{\sqrt{2}}(\|0\rangle + \|1\rangle)$	1	0.996
2	$\|0\rangle$	$\frac{1}{\sqrt{2}}(\|0\rangle + e^{\frac{i\pi}{4}}\|1\rangle)$	1	0.995
3	$\|0\rangle$	$\frac{1}{\sqrt{2}}(\|0\rangle + e^{\frac{i\pi}{2}}\|1\rangle)$	1	0.997
4	$\|0\rangle$	$\frac{1}{\sqrt{2}}(\|0\rangle + e^{i\pi}\|1\rangle)$	1	0.997
5	$\frac{1}{2}(\|0\rangle + \sqrt{3}\|1\rangle)$	$\frac{1}{2}(\sqrt{3}\|0\rangle + \|1\rangle)$	1	0.998
6	$\frac{1}{2}(\|0\rangle + e^{\frac{i\pi}{4}}\sqrt{3}\|1\rangle)$	$\frac{1}{2}(\sqrt{3}\|0\rangle + e^{\frac{i2\pi}{3}}\|1\rangle)$	1	0.974
7	$\frac{1}{2}(\|0\rangle + \sqrt{3}\|1\rangle)$	$\frac{1}{2}(\sqrt{3}\|0\rangle + \|1\rangle)$	2	0.999
8	$\frac{1}{2}(\|0\rangle + \sqrt{3}\|1\rangle)$	$\frac{1}{2}(\sqrt{3}\|0\rangle + \|1\rangle)$	3	0.999
9	$\frac{1}{2}(\|0\rangle + \sqrt{3}\|1\rangle)$	$\frac{e^{\frac{2\pi i}{3}}}{2}(\sqrt{3}\|0\rangle + \|1\rangle)$	1	0.999
10	$\frac{1}{2}(\|0\rangle + e^{\frac{i\pi}{4}}\sqrt{3}\|1\rangle)$	$\frac{e^{\frac{2\pi i}{3}}}{2}(\sqrt{3}\|0\rangle + e^{\frac{i2\pi}{3}}\|1\rangle)$	1	0.981
11	$\|0\rangle$	$\sin\frac{\pi}{36}\|0\rangle + \cos\frac{\pi}{36}\|1\rangle$	1	0.988

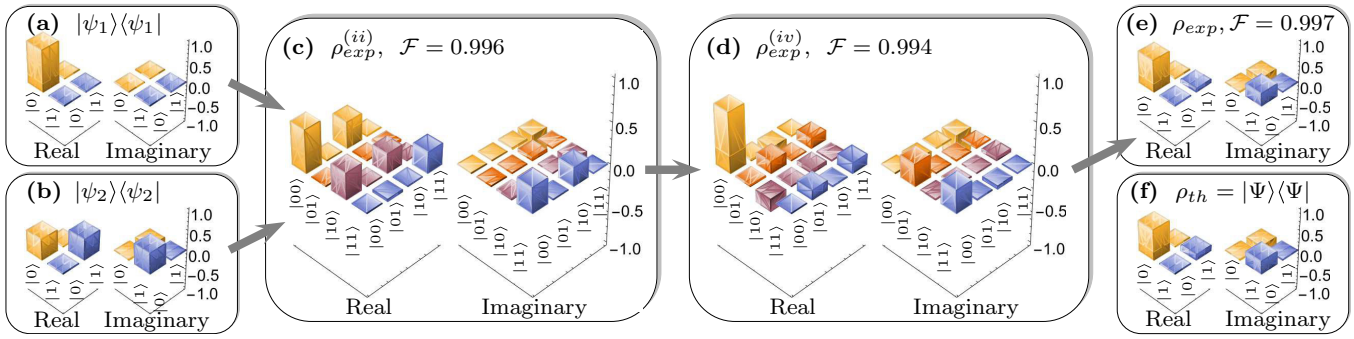

FIG. 2. (a)(b) The theoretical input states from dataset 3 of Table I; (c) the two-qubit state after encoding ($\rho_{\text{exp}}^{(ii)}$); (d) the state obtained at the end of step (iv) of the pulse sequence ($\rho_{\text{exp}}^{(iv)}$); (e),(f) the final experimentally obtained (ρ_{exp}) corresponding to step (v) and theoretically expected (ρ_{th}) single-qubit superposed states, respectively.

the experimentally superposed states and the theoretically expected ones. In the datasets numbered 1–4 of Table I, we have $|\psi_1\rangle = |0\rangle$ and $|\psi_2\rangle = \frac{1}{\sqrt{2}}(|0\rangle + e^{i\phi_2}|1\rangle)$, with $\phi_2 \in \{0, \frac{\pi}{4}, \frac{\pi}{2}, \pi\}$. Each of these pairs corresponds to the same two conical sections as per their Bloch sphere representations. Similarly, the datasets numbered 5 and 6 of Table I show the superposition between two pairs of states from the same respective conical sections. A detailed tomographic analysis corresponding to dataset 3 (Table I) is shown in Fig. 2. We also generated superpositions of the same constituent states with different weights, as given in datasets 5, 7, and 8 of Table I. For completeness, the experiments were performed with different overall phases of the input states. These phase factors were introduced while encoding the states $|\psi_1\rangle$ and $|\psi_2\rangle$ by applying a pulse of angle 2δ about the axis '$\hat{l}'$, which is aligned with the y axis at an angle $\pi + \gamma_2$ (Fig. 1). The encoded state is thus of the form $a|0\rangle|\psi_1\rangle + e^{i\gamma_2}b|1\rangle|\psi_2\rangle$. Experiments were performed for two pairs of states shown in datasets 9 and 10 in Table I. In both cases, $\gamma_2 = 120^\circ$ and the remaining parameters were the same as those of sets 5 and 6 in Table I. Now compare the datasets 5 with 9, and 6 with 10. As expected, the presence or absence of the overall phase does not affect the final superposed state. The efficacy of this experimental scheme does not directly depend upon the values of the overlaps ($|\langle\chi|\psi_i\rangle|$). This is evidenced by dataset 11 of Table I, where $|\psi_2\rangle$ is very close to $|\chi^\perp\rangle$ (orthogonal to $|\chi\rangle$). Table I shows that even if we choose the pair of input states $(|\psi_1\rangle, |\psi_2\rangle)$ outside the set $\{(|\psi_1\rangle, |\psi_2\rangle) : |\langle\chi|\psi_1\rangle| = \text{const}, |\langle\chi|\psi_2\rangle| = \text{const}\}$, our procedure still generates the expected superposition state $a|\psi_1\rangle + b|\psi_2\rangle$ with high accuracy.

IV. SUPERPOSITION OF MULTIPLE QUDITS

Our procedure can be readily extended to the superposition of arbitrary pure states of n qudits (d-dimensional quantum system) [4]. Let $a_1, a_2, \ldots, a_n$ be the desired coefficients for creating a superposition of n (d-dimensional) states $|\Psi_1\rangle_d, |\Psi_2\rangle_d, \ldots, |\Psi_n\rangle_d$. This requires a hybrid ($n \times d$)-dimensional qu$n$it-qudit system, where the qu$n$it (n-dimensional quantum system) acts as an ancilla (as before) and the qudit acts as the system. For simplicity, we use a vector representative $|\Psi\rangle_j$ to represent the set of states $e^{i\gamma_j}|\Psi\rangle_j$, where $\gamma_j \in [0, 2\pi]$. Consider now a d-dimensional referential state $|\chi\rangle_d$ whose nonzero overlaps, $|\langle\chi|\Psi_j\rangle_d|^2 = c_j$ ($j \in \{1, 2, \ldots, n\}$), are known. Following the same protocol as before, every qudit state is encoded in the $n \times d$ basis vectors of the hybrid qu$n$it-qudit system: $|j0\rangle, |j1\rangle, |j2\rangle, \ldots, |j(d-1)\rangle$, where $j \in \{0, 1, \ldots, n-1\}$. The phases of the constituent states are taken care of by using the information of overlaps of the respective constituent states with the referential state (see Appendix A). This is then followed by Fourier transformation of the qu$n$it, which is in fact the generalization of the Hadamard operation to higher-dimensional states [17]. The resultant state, which is a generalization of the two-qubit state in Eq. (4), is

$$\frac{1}{N\sqrt{n}} \sum_{j=0}^{n-1} \left(|j\rangle_n \otimes \sum_{k=1}^{n} (f^{j(k-1)} a_k |\Psi_k\rangle_d) \right), \tag{6}$$

where $f = e^{i\frac{2\pi}{n}}$ is the nth root of unity and N is the normalization constant. An arbitrary superposition of n pure states of a qudit is then obtained by the projective measurement $|0\rangle_n\langle 0|_n \otimes \mathbb{I}_{d\times d}$ subsequently tracing out the qu$n$it. The final state is a superposition of n d-dimensional states, which along with the information of overall phase factors of the constituent (n-qudits) states is (from Appendix A)

$$|\Psi\rangle = \frac{N_\Psi}{N\sqrt{n}} \sum_{k=1}^{n} a_k \left(\prod_{(j\neq k, j=1)}^{n} \frac{\langle\chi|\Psi_j\rangle_d}{\sqrt{c_j}} \right) |\Psi_k\rangle_d, \tag{7}$$

where N_Ψ is a constant that normalizes the un-normalized state obtained after the projective measurement. The superposed state $|\Psi\rangle$ [Eq. (7)] is obtained with the success probability

$$P = \frac{N_\Psi^2}{N^2 n} = \frac{\prod_{j=1}^{n} c_j}{\sum_{j=1}^{n} a_j^2 c_j} \frac{N_\Psi^2}{n}. \tag{8}$$

V. DISCUSSION

As per the superposition protocol discussed in Ref. [4], a projector $|\mu\rangle\langle\mu|$ (where $|\mu\rangle \propto \sqrt{c_1}|0\rangle + \sqrt{c_2}|1\rangle$) is applied on the first qubit to obtain the superposed state. It is discussed in [11] that precision of the implementation of this operator highly depends upon the values of $|\langle\chi|\psi_1\rangle|$ and $|\langle\chi|\psi_2\rangle|$. Smaller values of these overlaps lead to huge errors. Detailed analysis of this issue is carried out by Li *et al.* [11], where it is shown that when any of the overlap values ($|\langle\chi|\psi_1\rangle|, |\langle\chi|\psi_2\rangle|$) approaches zero, the protocol unexpectedly results in the final states with

poor fidelities. It has been clearly stated in Ref. [11] that the malfunctioning of the protocol, as $|\langle\chi|\psi_1\rangle|$ or $|\langle\chi|\psi_2\rangle| \to 0$, is mainly due to experimentally unavoidable imprecisions in the implementation of the $|\mu\rangle\langle\mu| \otimes I \otimes I$ projection operator. However, in the protocol implemented here, no such projector is used. Instead, we implement a Hadamard operator which, due to its ease to implement, neatly gives the resultant state. This is also reflected in one of our experimental results (Table I, dataset 11) where, despite the very small value of the overlap between the referential state and the constituent state, the experimental superimposed state is obtained with good fidelity. Thus the precision of our protocol is actually independent of the values of these overlaps, which makes this protocol more experimentally feasible.

A closer analysis of the success probabilities obtained in different superposition protocols and for different amount of prior information is given in following sections.

A. Comparison between general two-qubit- and three-qubit-based implementations

In this section, we compare the success probabilities obtained in our scheme with that of a previously implemented scheme [4,11] to carry out the superposition of two single-qubit states. For the purpose of comparison, we start with same amount of resources. Thus we use the protocol discussed in Sec. II to obtain the present two-qubit-based scheme from the existing three-qubit-based scheme [4] to superimpose two single-qubit pure states. Recalling Eq. (A7), the resultant superposed state is given as

$$\sqrt{\frac{c_1c_2}{2(c_1|a|^2+c_2|b|^2)}}\left(a\frac{\langle\chi|\psi_2\rangle}{|\langle\chi|\psi_2\rangle|}|\psi_1\rangle+b\frac{\langle\chi|\psi_1\rangle}{|\langle\chi|\psi_1\rangle|}|\psi_2\rangle\right). \tag{9}$$

The success probability in this case is given as $P_2 = \frac{c_1c_2}{2(c_1|a|^2+c_2|b|^2)}N_\psi^2$. Here, N_ψ is the normalization factor for state $a|\psi_1\rangle + b|\psi_2\rangle$ (where $\sqrt{|a|^2+|b|^2}=1$). Recalling the treatment in a three-qubit-based protocol [4,11], the resultant state in that case is given as

$$\sqrt{\frac{c_1c_2}{c_1+c_2}}\left(a\frac{\langle\chi|\psi_2\rangle}{|\langle\chi|\psi_2\rangle|}|\psi_1\rangle+b\frac{\langle\chi|\psi_1\rangle}{|\langle\chi|\psi_1\rangle|}|\psi_2\rangle\right). \tag{10}$$

The success probability in this case is $P_3 = \frac{c_1c_2}{c_1+c_2}N_\psi^2$. Comparing the success probabilities resulting from these two protocols, we have

$$r_p = \frac{P_2}{P_3} = \frac{c_1+c_2}{2(c_1|a|^2+c_2|b|^2)} = \frac{r_c+1}{2[1+|b|^2(r_c-1)]}, \tag{11}$$

where $r_c = \frac{c_2}{c_1} \in (0,\infty)$, $|a|^2,|b|^2 \in (0,1)$, and $r_p \in (0,\infty)$. The same value of success probabilities (P_2 and P_3) results in the case in which the overlaps $c_1 = c_2$ or the superposition is obtained with equal weights, i.e., $|a|^2 = |b|^2$. Figure 3 shows the variation r_p vs r_c at different values of $|b|^2$. It is interesting to note that our two-qubit-based protocol outperforms the three-qubit-based protocol (in terms of success probabilities) in the range $0.5 < |b|^2 < 1$ (when $0 < r_c < 1$) and in the range $0 < |b|^2 < 0.5$ (when $1 < r_c < \infty$). With reference to Table I, experimental dataset 7 has $r_c = 3$, $|b|^2 = 0.2$ and dataset 8 corresponds to $r_c = 3$, $|b|^2 = 0.1$, which correspond to $r_p > 1$ as per Fig. 3.

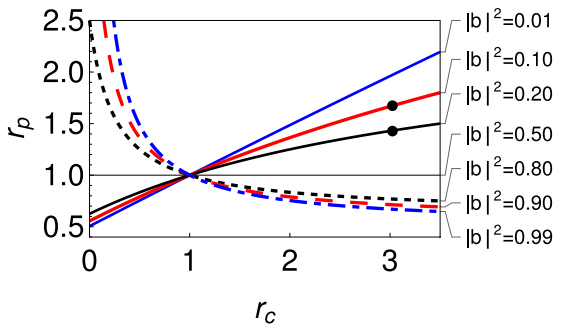

FIG. 3. The variation of $r_p = P_2/P_3$ is shown with the ratio of overlaps, with $r_c = c_2/c_1$ corresponding to different values of $|b|^2$. Different curves correspond to different values of $|b|^2$, which are specified on the right side of the plot. Two black points on the curves for $|b|^2 = 0.1, 0.2$ correspond to experimental conditions of datasets 7 and 8 of Table I.

B. Enhancement in success probability subject to prior information

In general, there is an interplay between the success probability with which the desired superposed state is obtained and the amount of prior information regarding constituent states. We impose certain constraints on the constituent states and observe its impact on the success probabilities. Reconsidering the problem of superposition of two single-qubit states having fixed nonzero overlaps, $|\langle\chi|\psi_1\rangle|^2 = c_1$ and $|\langle\chi|\psi_2\rangle|^2 = c_2$, with the referential state $|\chi\rangle$ [4], we have $|\langle\chi^\perp|\psi_1\rangle|^2 = c_1^\perp = 1 - c_1$ and $|\langle\chi^\perp|\psi_2\rangle|^2 = c_2^\perp = 1 - c_2$, where $\langle\chi|\chi^\perp\rangle = 0$. In this case, we consider the action of the identity operator $U_1 = I \otimes I \otimes (|\chi\rangle\langle\chi| + |\chi^\perp\rangle\langle\chi^\perp|)$ (instead of $I \otimes I \otimes |\chi\rangle\langle\chi|$). Using the overlaps of the input states with both $|\chi\rangle$ and $|\chi^\perp\rangle$, we observe an increase in the success probability (see Appendix B). Further, we implement the single-qubit unitary operator U_χ ($U_{\chi^\perp}$) on the first qubit, if the third qubit is in state $|\chi\rangle$ ($|\chi^\perp\rangle$) (see Appendix B for details). The explicit forms of the operators are

$$U_\chi = \frac{1}{N_1}\begin{pmatrix}\frac{1}{\sqrt{c_1}} & \frac{1}{\sqrt{c_2}}\\ \frac{1}{\sqrt{c_2}} & \frac{-1}{\sqrt{c_1}}\end{pmatrix}, \quad U_{\chi^\perp} = \frac{1}{N_2}\begin{pmatrix}\frac{1}{\sqrt{c_1^\perp}} & \frac{1}{\sqrt{c_2^\perp}}\\ \frac{1}{\sqrt{c_2^\perp}} & \frac{-1}{\sqrt{c_1^\perp}}\end{pmatrix},$$

where $N_1 = \sqrt{(c_1+c_2)/c_1c_2}$, $N_2 = \sqrt{(c_1^\perp+c_2^\perp)/c_1^\perp c_2^\perp}$. In this formalism, we mainly study two types of constraints, in which both $|\psi_1\rangle$ and $|\psi_2\rangle$ lie in the (i) same longitudinal plane and the (ii) same transverse plane of the Bloch sphere, In case (i), the desired superposed state is obtained with success probability

$$P^{\rm tot} = N_\psi^2\left(\frac{c_1c_2}{c_1+c_2}+\frac{c_1^\perp c_2^\perp}{c_1^\perp+c_2^\perp}\right) = P_3+N_\psi^2\frac{c_1^\perp c_2^\perp}{c_1^\perp+c_2^\perp}. \tag{12}$$

For $c_1 = c_2^\perp$, the success probability $P^{\rm tot} = 2P_3$ becomes double that of the ordinary case. In case (ii), we have $c_1 = c_2 = c$ (say), which implies $c_1^\perp = c_2^\perp = c^\perp$ (say). Further, assuming both states occupy diametrically opposite positions on the respective spherical sections of the Bloch sphere, the total

success probability obtained then is given by

$$P^{\text{tot}} = N_\psi^2\left(\frac{c}{2}+\frac{c^\perp}{2}\right)=\frac{1}{2}N_\psi^2, \tag{13}$$

which is again greater than P_3. Further, if both states lie in the equatorial plane, this pair of states becomes orthogonal and the success probability reaches 1/2. Equations (12) and (A6) give higher success probabilities (for certain a,b values) compared to the a,b-dependent protocol discussed in Ref. [4]. Recently, we came across a different approach [18], analyzing the superposition of an arbitrary pair of orthogonal states.

VI. CONCLUSIONS

We have experimentally created a superposition of single-qubit states in the defined framework, covering all possible aspects, i.e., (i) creation of various single-qubit states and obtaining their superposition, (ii) superposition with arbitrary weights, and (iii) superposition of single-qubit states in the presence of assumed overall phases. All the experimental results have been obtained with fidelities over 0.97. This protocol has also been extended for the superposition of multiple states of a qudit. We have also discussed certain special cases where the desired superposed state is obtained with enhanced success probability.

ACKNOWLEDGMENTS

S.D. acknowledges the financial support by The Institute of Mathematical Sciences, Chennai, India, and the Technische Universität Dortmund, Germany, and is supported by the International Collaborative Research Centre TRR 160 "Coherent manipulation of interacting spin excitations in tailored semiconductors," funded by the Deutsche Forschungsgemeinschaft. S.D., G.T., and S.G. would like to thank Somshubhro Bandyopadhyay, Manik Banik, Prathik Cherian J., Guruprasad Kar, Samir Kunkri, and Ramij Rahaman for useful discussions.

APPENDIX A: ENCODING SCHEME

Let us discuss the case of the superposition of an n number of pure states of a qudit. Consider a d-dimensional referential state $|\chi\rangle_d$, whose overlap (magnitude) with each of the constituent states is known. Therefore, assume $|\langle\chi|\Psi_j\rangle_d|^2 = c_j$, where $j \in \{1,2,\ldots,n\}$. Let $a_1,a_2,\ldots,a_n$ be the desired weights for creating a superposition of d-dimensional states $|\Psi_1\rangle_d,|\Psi_2\rangle_d,\ \ldots,|\Psi_n\rangle_d$, respectively. We begin with the initial state,

$$\frac{1}{N}(a_1'|0\rangle_n + a_2'|1\rangle_n + \cdots + a_n'|n-1\rangle_n) \otimes|\Psi_1\rangle_d\otimes\cdots\otimes|\Psi_n\rangle_d, \tag{A1}$$

where N is the normalization factor, which is equal to $\sqrt{\sum_{j=1}^n a_j'^2}$. This state belongs to a $[n\times(d)^n]$-dimensional Hilbert space, where the primed coefficients are

$$a_k' = \frac{a_k}{\prod_{(j\neq k,j=1)}^n|\langle\chi|\Psi_j\rangle_d|} = \frac{a_k}{\sqrt{\prod_{(j\neq k,j=1)}^n c_j}}. \tag{A2}$$

This initial state is then made to undergo a series of controlled-SWAP operations, $\mathcal{CS}_{2,3}^1\mathcal{CS}_{2,4}^1\ldots\mathcal{CS}_{2,n}^1$, where the state of the first spin acts as the control. In order to describe the action of this operation, let us reconsider the set of bases vectors of the control spin ($|k\rangle_n, k\in\{0,1,\ldots,n-1\}$) in n-dimensional Hilbert space; whenever the first spin (qu$n$it) is in state $|k\rangle_n$, states of the first qudit (second spin) and the $(k+1)$th qudit [$(k+2)$th spin] get swapped. The resulting state is of the form

$$\frac{1}{N}(a_1'|0\rangle_n\otimes|\Psi_1\rangle_d\otimes|\Psi_2\rangle_d\otimes\cdots\otimes|\Psi_n\rangle_d + a_2'|1\rangle_n\otimes|\Psi_2\rangle_d\otimes|\Psi_1\rangle_d\otimes\cdots\otimes|\Psi_n\rangle_d+\cdots + a_n'|n-1\rangle_n\otimes|\Psi_n\rangle_d\otimes|\Psi_3\rangle_d\otimes\cdots\otimes|\Psi_1\rangle_d). \tag{A3}$$

This is then acted upon by a set of projection operators constructed using the referential state $|\chi\rangle_d$. The operator performing the $n-1$ number of projections on qudits numbered 2 to n (or spins numbered 3 to $n+1$ in the 1-qu$n$it $\otimes$ n-qudit system) is given as $I_{n\times n}\otimes I_{d\times d}\otimes\bigotimes_{k=2}^n(|\chi\rangle_d\langle\chi|_d)_k$, where k represents the qudit number. This helps to remove the phases that may be occurring with the constituent states ($|\Psi\rangle_d$'s). The resulting state is given as

$$\frac{1}{N}\sum_{k=1}^n\left[a_k\left(\prod_{(j\neq k,j=1)}^n\frac{\langle\chi|\Psi_j\rangle_d}{\sqrt{c_j}}\right)|k-1\rangle_n|\Psi_k\rangle_d\right]\bigotimes_{m=1}^{n-1}|\chi\rangle_d. \tag{A4}$$

Tracing out states of qudits numbered 2 to n, we are left with a $(n\times d)$-dimensional state. Also, shedding the overall phases, the state in Eq. (A4) is written in a simple manner,

$$\frac{1}{N}(a_1|0\rangle_n|\Psi_1\rangle_d + a_2|1\rangle_n|\Psi_2\rangle_d+\cdots+a_n|n-1\rangle_n|\Psi_n\rangle_d), \tag{A5}$$

where $N=\sqrt{\sum_{i=1}^n|a_i'|^2}$. In the case of superposition of two qubits with weights $a_1=a$ and $a_2=b$, the above equation is reduced to

$$\frac{1}{N}\left(a\frac{\langle\chi|\Psi_2\rangle}{|\langle\chi|\Psi_2\rangle|}|0\rangle\otimes|\Psi_1\rangle + b\frac{\langle\chi|\Psi_1\rangle}{|\langle\chi|\Psi_1\rangle|}|1\rangle\otimes|\Psi_2\rangle\right). \tag{A6}$$

This is the two-qubit encoded state, which, after Hadamard implementation on the first qubit followed by a projection operator $|0\rangle\langle0|\otimes I$, gives rise to the expected superposed state given as

$$\frac{1}{\sqrt{2}N}\left(a\frac{\langle\chi|\Psi_2\rangle}{|\langle\chi|\Psi_2\rangle|}|\Psi_1\rangle + b\frac{\langle\chi|\Psi_1\rangle}{|\langle\chi|\Psi_1\rangle|}|\Psi_2\rangle\right). \tag{A7}$$

The additional factor $\frac{1}{N}=\sqrt{\frac{c_1c_2}{c_1|a|^2+c_2|b|^2}}$. Thus we reduce the existing three-qubit-based protocol described in [4] to the present two-qubit-based protocol described in the main text. It is to be noted that the state given by Eq. (A6) has already taken care of the overall phases of states $|\Psi_1\rangle$ and $|\Psi_2\rangle$.

APPENDIX B: PRIOR INFORMATION AND SUCCESS PROBABILITIES

There is an interplay between the amount of prior information needed to superimpose a pair of partially known single-qubit pure states and the success probability with which the resultant superposed state is obtained. In this appendix, we

discuss the superposition protocol for a pair of single-qubit pure states under additional constraints that further leads to enhanced success probability. We reconsider the problem of superposition of two arbitrary single-qubit states with known nonzero overlaps, $|\langle\chi|\psi_1\rangle|^2 = c_1$ and $|\langle\chi|\psi_2\rangle|^2 = c_2$, with the referential single-qubit state $|\chi\rangle$. Thus one can obtain the overlaps of the constituent states with $|\chi^\perp\rangle$ (single-qubit state orthogonal to $|\chi\rangle$). We have $|\langle\chi^\perp|\psi_1\rangle|^2 = c_1^\perp = 1 - c_1$ and $|\langle\chi^\perp|\psi_2\rangle|^2 = c_2^\perp = 1 - c_2$. Let us begin with a three-qubit initial state, similar to the one given in Eq. (A1),

$$(a|0\rangle + b|1\rangle) \otimes |\psi_1\rangle \otimes |\psi_2\rangle. \tag{B1}$$

This state is then acted upon by the same three-qubit controlled-SWAP operation as described in Appendix A, such that the resulting state is

$$a|0\rangle \otimes |\psi_1\rangle \otimes |\psi_2\rangle + b|1\rangle \otimes |\psi_2\rangle \otimes |\psi_1\rangle. \tag{B2}$$

Consider the action of the identity operator $U_1 = I \otimes I \otimes (|\chi\rangle\langle\chi| + |\chi^\perp\rangle\langle\chi^\perp|)$ on the three-qubit state given in Eq. (B1). The resultant state is given as

$$\begin{aligned}&[a\langle\chi|\psi_2\rangle|0\rangle|\psi_1\rangle + b\langle\chi|\psi_1\rangle|1\rangle|\psi_2\rangle] \otimes |\chi\rangle \\ &+ [a\langle\chi^\perp|\psi_2\rangle|0\rangle|\psi_1\rangle + b\langle\chi^\perp|\psi_1\rangle|1\rangle|\psi_2\rangle] \otimes |\chi^\perp\rangle.\end{aligned} \tag{B3}$$

Another controlled unitary operation is implemented on the first qubit, where the state of the third qubit acts as the control. Subject to the state of the third qubit ($|\chi\rangle$ or $|\chi^\perp\rangle$), the action of this controlled operation (on the first qubit) is described as

$$\begin{aligned}U_{|\chi\rangle}|0\rangle &\to \frac{1}{N_1}\left(\frac{1}{\sqrt{c_2}}|0\rangle + \frac{1}{\sqrt{c_1}}|1\rangle\right), \\ U_{|\chi\rangle}|1\rangle &\to \frac{1}{N_1}\left(\frac{1}{\sqrt{c_1}}|0\rangle - \frac{1}{\sqrt{c_2}}|1\rangle\right), \\ U_{|\chi^\perp\rangle}|0\rangle &\to \frac{1}{N_2}\left(\frac{1}{\sqrt{c_2^\perp}}|0\rangle + \frac{1}{\sqrt{c_1^\perp}}|1\rangle\right), \\ U_{|\chi^\perp\rangle}|1\rangle &\to \frac{1}{N_2}\left(\frac{1}{\sqrt{c_1^\perp}}|0\rangle - \frac{1}{\sqrt{c_2^\perp}}|1\rangle\right),\end{aligned} \tag{B4}$$

where

$$\frac{1}{N_1} = \sqrt{\frac{c_1 c_2}{c_1 + c_2}} \quad \text{and} \quad \frac{1}{N_2} = \sqrt{\frac{c_1^\perp c_2^\perp}{c_1^\perp + c_2^\perp}}.$$

Equation (B3) thus leads to

$$\begin{aligned}&\frac{a}{N_1}\left(\frac{\langle\chi|\psi_2\rangle}{\sqrt{c_2}}|0\rangle + \frac{\langle\chi|\psi_2\rangle}{\sqrt{c_1}}|1\rangle\right)|\psi_1\rangle \otimes |\chi\rangle \\ &+ \frac{b}{N_1}\left(\frac{\langle\chi|\psi_1\rangle}{\sqrt{c_1}}|0\rangle - \frac{\langle\chi|\psi_1\rangle}{\sqrt{c_2}}|1\rangle\right)|\psi_2\rangle \otimes |\chi\rangle \\ &+ \frac{a}{N_2}\left(\frac{\langle\chi^\perp|\psi_2\rangle}{\sqrt{c_2^\perp}}|0\rangle + \frac{\langle\chi^\perp|\psi_2\rangle}{\sqrt{c_1^\perp}}|1\rangle\right)|\psi_1\rangle \otimes |\chi^\perp\rangle \\ &+ \frac{b}{N_2}\left(\frac{\langle\chi^\perp|\psi_1\rangle}{\sqrt{c_1^\perp}}|0\rangle - \frac{\langle\chi^\perp|\psi_1\rangle}{\sqrt{c_2^\perp}}|1\rangle\right)|\psi_2\rangle \otimes |\chi^\perp\rangle.\end{aligned} \tag{B5}$$

Application of the projection operator $|0\rangle\langle 0| \otimes I_{2\times 2} \otimes I_{2\times 2}$ then leads to

$$\begin{aligned}&\frac{1}{N_1}\left(a\frac{\langle\chi|\psi_2\rangle}{|\langle\chi|\psi_2\rangle|}|\psi_1\rangle + b\frac{\langle\chi|\psi_1\rangle}{|\langle\chi|\psi_1\rangle|}|\psi_2\rangle\right) \otimes |\chi\rangle \\ &+ \frac{1}{N_2}\left(a\frac{\langle\chi^\perp|\psi_2\rangle}{|\langle\chi^\perp|\psi_2\rangle|}|\psi_1\rangle + b\frac{\langle\chi^\perp|\psi_1\rangle}{|\langle\chi^\perp|\psi_1\rangle|}|\psi_2\rangle\right) \otimes |\chi^\perp\rangle.\end{aligned} \tag{B6}$$

Thus we obtain the weighted superpositions of single-qubit states $|\psi_1\rangle$ and $|\psi_2\rangle$. If the state of the second qubit here is $|\chi\rangle$, then the superposed state

$$|\Psi^{(1)}\rangle = \frac{N_\psi^{(1)}}{N_1}\left(a\frac{\langle\chi|\psi_2\rangle}{|\langle\chi|\psi_2\rangle|}|\psi_1\rangle + b\frac{\langle\chi|\psi_1\rangle}{|\langle\chi|\psi_1\rangle|}|\psi_2\rangle\right) \tag{B7}$$

is obtained with a success probability $P^{(1)} = (N_\psi^{(1)})^2 \frac{c_1 c_2}{c_1 + c_2}$. While corresponding to the second-qubit state $|\chi^\perp\rangle$, the superposed state

$$|\Psi^{(2)}\rangle = \frac{N_\psi^{(2)}}{N_2}\left(a\frac{\langle\chi^\perp|\psi_2\rangle}{|\langle\chi^\perp|\psi_2\rangle|}|\psi_1\rangle + b\frac{\langle\chi^\perp|\psi_1\rangle}{|\langle\chi^\perp|\psi_1\rangle|}|\psi_2\rangle\right) \tag{B8}$$

is obtained with a success probability $P^{(2)} = (N_\psi^{(2)})^2 \frac{c_1^\perp c_2^\perp}{c_1^\perp + c_2^\perp}$. $N_\psi^{(1)}$ and $N_\psi^{(2)}$ are the normalization factors of the first-qubit state when states of the second qubit are $|\chi\rangle$ and $|\chi^\perp\rangle$, respectively, in Eq. (B6). States given in Eqs. (B7) and (B8) are weighted superpositions of the same constituent states $|\psi_1\rangle$ and $|\psi_2\rangle$. But they may be different because of their possibly different relative phases. The situation of our interest arises when $|\Psi^{(1)}\rangle$ varies from $|\Psi^{(2)}\rangle$ only up to a global phase. Following are a few special cases discussing such scenarios.

1. Both states belong to the same longitudinal plane on the Bloch sphere

Assume now that both $|\psi_1\rangle$ and $|\psi_2\rangle$ lie in the same longitudinal plane on the Bloch sphere, as shown in Fig. 4. More explicitly, for $\frac{\langle\chi^\perp|\psi_j\rangle}{|\langle\chi^\perp|\psi_j\rangle|} = e^{\iota\phi}\frac{\langle\chi|\psi_j\rangle}{|\langle\chi|\psi_j\rangle|}$, Eq. (B6) takes the form

$$\left(a\frac{\langle\chi|\psi_2\rangle}{|\langle\chi|\psi_2\rangle|}|\psi_1\rangle + b\frac{\langle\chi|\psi_1\rangle}{|\langle\chi|\psi_1\rangle|}|\psi_2\rangle\right) \otimes \left(\frac{1}{N_1}|\chi\rangle + \frac{e^{\iota\phi}}{N_2}|\chi^\perp\rangle\right). \tag{B9}$$

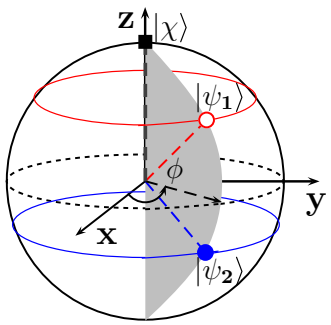

FIG. 4. Bloch sphere representation of $|\psi_1\rangle, |\psi_2\rangle$, and $|\chi\rangle$, marked with an unfilled red circle, filled blue circle, and filled black square, respectively.

Tracing out the second qubit, we obtain

$$\sqrt{\frac{1}{N_1^2}+\frac{1}{N_2^2}}N_\psi\left(a\frac{\langle\chi|\psi_2\rangle}{|\langle\chi|\psi_2\rangle|}|\psi_1\rangle+b\frac{\langle\chi|\psi_1\rangle}{|\langle\chi|\psi_1\rangle|}|\psi_2\rangle\right), \quad \text{(B10)}$$

which is the desired superposed state. This superposed state is obtained with success probability

$$P^{\text{tot}} = N_\psi^2\left(\frac{c_1c_2}{c_1+c_2}+\frac{c_1^\perp c_2^\perp}{c_1^\perp+c_2^\perp}\right) = P_3 + N_\psi^2\frac{c_1^\perp c_2^\perp}{c_1^\perp+c_2^\perp}. \quad \text{(B11)}$$

This can as well be written as $P^{\text{tot}} = P + P^\perp$, where $P = (\frac{N_\psi}{N_1})^2$ and $P^\perp = (\frac{N_\psi}{N_2})^2$. Putting another constraint, $c_1 = c_2^\perp$, we obtain $N_1 = N_2$, which gives rise to the desired superposed state with a success probability

$$P^{\text{tot}} = 2N_\psi^2\frac{c_1c_2}{c_1+c_2} = 2P. \quad \text{(B12)}$$

2. Both states belong to the same transverse plane on the Bloch sphere

In this case, we have $c_1 = c_2 = c$ (say), which implies $c_1^\perp = c_2^\perp = c^\perp$ (say). Equation (B5) thus leads to

$$\begin{aligned}&\frac{1}{N}|0\rangle\left(a\frac{\langle\chi|\psi_2\rangle}{\sqrt{c}}|\psi_1\rangle+b\frac{\langle\chi|\psi_1\rangle}{\sqrt{c}}|\psi_2\rangle\right)\otimes|\chi\rangle\\&+\frac{1}{N}|1\rangle\left(a\frac{\langle\chi|\psi_2\rangle}{\sqrt{c}}|\psi_1\rangle-b\frac{\langle\chi|\psi_1\rangle}{\sqrt{c}}|\psi_2\rangle\right)\otimes|\chi\rangle\\&+\frac{1}{N}|0\rangle\left(a\frac{\langle\chi^\perp|\psi_2\rangle}{\sqrt{c^\perp}}|\psi_1\rangle+b\frac{\langle\chi^\perp|\psi_1\rangle}{\sqrt{c^\perp}}|\psi_2\rangle\right)\otimes|\chi^\perp\rangle\\&+\frac{1}{N}|1\rangle\left(a\frac{\langle\chi^\perp|\psi_2\rangle}{\sqrt{c^\perp}}|\psi_1\rangle-b\frac{\langle\chi^\perp|\psi_1\rangle}{\sqrt{c^\perp}}|\psi_2\rangle\right)\otimes|\chi^\perp\rangle.\end{aligned} \quad \text{(B13)}$$

Further, assuming both states occupy diametrically opposite positions on the respective spheric sections of the Bloch sphere, the azimuthal angles of the two states may be considered as ϕ and $\pi+\phi$. Under the action of projection operator $|0\rangle\langle 0|\otimes I\otimes|\chi\rangle\langle\chi|$, Eq. (B13) gives rise to the desired superposed state

$$\frac{1}{N_1}\left(a\frac{\langle\chi|\psi_2\rangle}{\sqrt{c}}|\psi_1\rangle+b\frac{\langle\chi|\psi_1\rangle}{\sqrt{c}}|\psi_2\rangle\right) \quad \text{(B14)}$$

with a success probability $P = (\frac{N_\psi}{N_1})^2$. Note that with the projection operator $|1\rangle\langle 1|\otimes I\otimes|\chi^\perp\rangle\langle\chi^\perp|$, Eq. (B13) gives rise to the desired superposed state

$$\frac{1}{N_2}\left(a\frac{\langle\chi^\perp|\psi_2\rangle}{\sqrt{c^\perp}}|\psi_1\rangle+b\frac{\langle\chi^\perp|\psi_1\rangle}{\sqrt{c^\perp}}|\psi_2\rangle\right) \quad \text{(B15)}$$

with a success probability $P^\perp = (\frac{N_\psi}{N_2})^2$. The total success probability obtained in the above two instances is

$$P^{\text{tot}} = P + P^\perp = N_\psi^2\left(\frac{1}{N_1^2}+\frac{1}{N_2^2}\right) = \frac{1}{2}N_\psi^2. \quad \text{(B16)}$$

Further, if both states lie in the equatorial plane, this pair of states becomes orthogonal and the success probability reaches 1/2. Equations (B11) and (B16) give higher success probabilities (for certain a,b values) compared to the a,b-dependent protocol discussed in the supplemental material of Ref. [4].

[1] P. A. M. Dirac, *The Principles of Quantum Mechanics* (Clarendon Press, Oxford, 1930).

[2] N. D. H. Dass, arXiv:1311.4275.

[3] U. Alvarez-Rodriguez, M. Sanz, L. Lamata, and E. Solano, Sci. Rep. **5**, 11983 (2015).

[4] M. Oszmaniec, A. Grudka, M. Horodecki, and A. Wójcik, Phys. Rev. Lett. **116**, 110403 (2016).

[5] L. Lamata, U. Alvarez-Rodriguez, J. D. Martín-Guerrero, M. Sanz, and E. Solano, arXiv:1709.07409.

[6] M. A. Nielsen and I. L. Chuang, *Quantum Computation and Quantum Information* (Cambridge University Press, Cambridge, 2000).

[7] J. Stolze and D. Suter, *Quantum Computing: A Short Course from Theory to Experiment* (Wiley-VCH Verlag, Berlin, 2004).

[8] J. Stolze and D. Suter, *Quantum Computing, Revised and Enlarged* (Wiley-VCH Verlag, Berlin, 2008).

[9] T. D. Ladd, F. Jelezko, R. Laflamme, Y. Nakamura, C. Monroe, and J. L. O'Brien, Nature (London) **464**, 45 (2010).

[10] X.-M. Hu, M.-J. Hu, J.-S. Chen, B.-H. Liu, Y.-F. Huang, C.-F. Li, G.-C. Guo, and Y.-S. Zhang, Phys. Rev. A **94**, 033844 (2016).

[11] K. Li, G. Long, H. Katiyar, T. Xin, G. Feng, D. Lu, and R. Laflamme, Phys. Rev. A **95**, 022334 (2017).

[12] R. Li, U. Alvarez-Rodriguez, L. Lamata, and E. Solano, Quantum Meas. Quantum Metrol. **4**, 1 (2017).

[13] J. Thompson, K. Modi, V. Vedral, and M. Gu, New J. Phys. **20**, 013004 (2018).

[14] M. Araújo, A. Feix, F. Costa, and Časlav Brukner, New J. Phys. **16**, 093026 (2014).

[15] N. Friis, V. Dunjko, W. Dür, and H. J. Briegel, Phys. Rev. A **89**, 030303 (2014).

[16] D. G. Cory, M. D. Price, and T. F. Havel, Physica D: Nonlinear Phenom. **120**, 82 (1998).

[17] S. Dogra, Arvind, and K. Dorai, Int. J. Quantum Inf. **13**, 1550059 (2015).

[18] M. Doosti, F. Kianvash, and V. Karimipour, Phys. Rev. A **96**, 052318 (2017).